DOI: 10.1002/ejic.200600262

# Synthesis, Structures, and Luminescent Properties of $d^{10}$ Group 12 Metal Complexes with Substituted 2,2′-Bipyridine Ligands

**Xiao-ming Liu,[a] Xiao-yue Mu,[a] Hong Xia,[a,b] Ling Ye,[a] Wei Gao,[a] Hao-yu Wang,[a] and Ying Mu*[a]**

**Keywords:** Group 12 metal complexes / 2,2′-Bipyridine / Solid-state structures / Luminescence

Four $d^{10}$ group 12 metal complexes, 6-(2-methoxyphenyl)-2,2′-bipyridinezinc dichloride (**2a**), -mercury dichloride (**2b**), 6-[2-(dimethylamino)phenyl]-2,2′-bipyridinezinc dichloride (**2c**), and -mercury dichloride (**2d**), were synthesized and the structures determined by single-crystal X-ray crystallography. Complexes **2a** and **2b** are four-coordinate and adopt a distorted tetrahedral geometry, while complexes **2c** and **2d** are five-coordinate with a distorted trigonal bipyramidal geometry for the metal center. Luminescent properties of complexes **2a**–**2d** in both solution and the solid state were studied.



## Introduction

Luminescent coordination complexes have attracted increasing attention because of their potential application in areas of optoelectronic devices and chemical sensors.[1] One of the most important considerations in organic light-emitting diodes (OLEDs) is the design and synthesis of molecules capable of tuning luminescent properties through the modification of ligands.[2,3] The organic compounds with aromatic nitrogen heterocycles, which can be receptors for metal ions, have been studied extensively because they are capable of performing useful light- and/or redox-induced tasks. For example, a large number of complexes based on 8-hydroxyquinoline, 7-azaindole, pyridyl-phenol, and phenyl-pyridine have been investigated during the last decades.[3–5] Particularly, luminescent complexes of $Re^{I}$,[6] $Ru^{II}$,[7] and $Os^{II}$[8] containing bipyridine type ligands have attracted much attention because of their high luminescent efficiency. However, the lower synthetic yields and higher costs of these complexes are disadvantages for their use as optoelectronic materials. The lower-cost $d^{10}$ metal complexes with the nitrogen-containing ligands are of interest because of their photoluminescent and/or electroluminescent properties.[9–11] To develop new complexes of this type with improved luminescent performance, we have synthesized four new complexes of zinc(II) and mercury(II) with modified bipyridine ligands that are synthesized by introducing an aromatic group with a donor at its α position to the 3-position of 2,2′-bipyridine. The ligands were selected considering that larger conjugating systems can be formed in their complexes and better luminescent properties might be expected. We herein report on the preparation, structural characterization, and photoluminescence of these zinc(II) and mercury(II) complexes.

[a] Key Laboratory for Supramolecular Structure and Materials of Ministry of Education, School of Chemistry, Jilin University, 2699 Qianjin Street, Changchun 130012, People's Republic of China
Fax: +86-431-5193421
E-mail: ymu@mail.jlu.edu.cn
[b] State Key Laboratory of Integrated Optoelectronics, College of Electronic Science and Technology, Jilin University, Changchun 130012, People's Republic of China

## Results and Discussion

### Synthesis of Compounds

Ligand **1a** was prepared according to a known procedure (Scheme 1)[12] and ligand **1b** was synthesized by the reaction of dry 2,2′-bipyridine with the aryllithium reagent, obtained from the treatment of 2-bromo-*N*,*N*-dimethylaniline with *n*BuLi, in moderate yield after oxidative rearomatization. Ligand **1a** is a known compound while **1b** is a new compound. The new ligand **1b** was characterized by $^1$H NMR spectroscopy along with elemental analysis. The $^1$H NMR spectrum of **1b** exhibits resonance at $\delta$ = 2.77 ppm for the $CH_3$ proton. Compound **1b** is soluble in most organic solvents. Treatment of $ZnCl_2$ and $HgCl_2$ with equivalent free ligands in methanol at ambient temperature afforded the corresponding $d^{10}$ metal complexes **2a**–**2d** in good yields (>80%) as light yellow or white crystalline solids (Scheme 1). Complexes **2a**–**2d** were all characterized by elemental analyses, $^1$H NMR spectroscopy, and IR spectroscopy, and satisfactory analytic results were obtained on all compounds. All complexes are moderately soluble in DMSO, slightly soluble in dichloromethane, methanol, DMF, and THF, and insoluble in saturated hydrocarbon solvents.

  

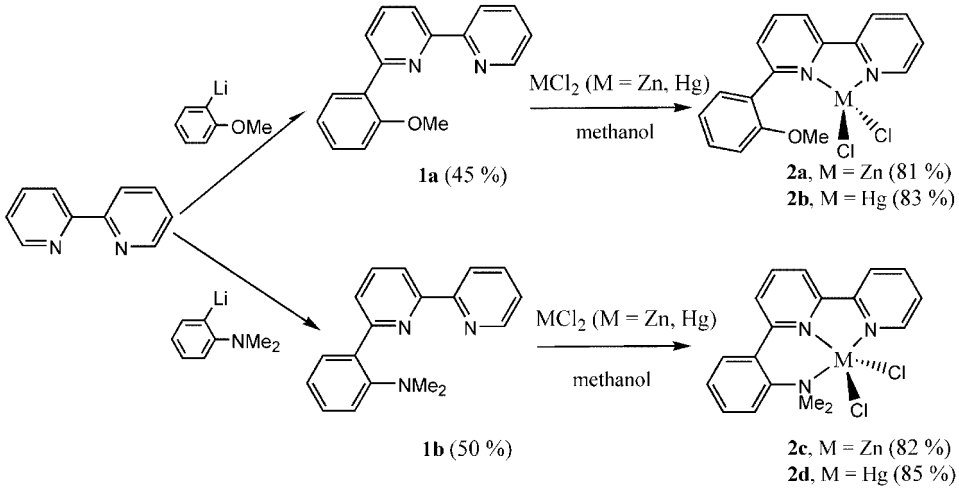


Scheme 1. Synthetic procedure of ligands **1a** and **1b**, and of complexes **2a**–**2d**.

### Crystal Structure

The molecular structures of complexes **2a**, **2b**, **2c**, and **2d** were determined by X-ray crystallographic analysis. Crystals of all four complexes suitable for X-ray crystal structure

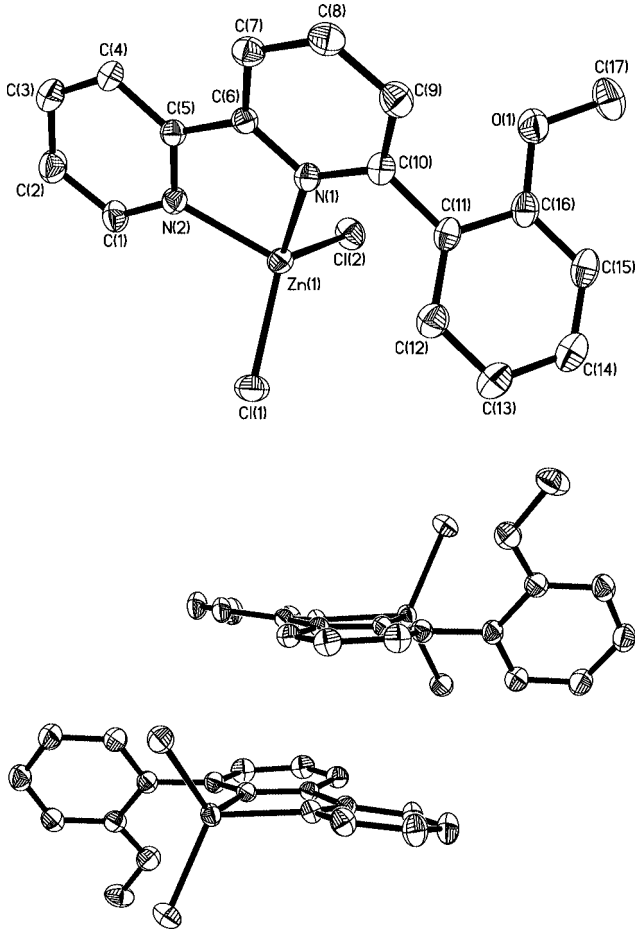


Figure 1. Top: molecular structure of complex **2a**; bottom: crystal packing diagram between two adjacent molecules of **2a** showing the lack of a π–π stacking interaction in the solid state. (Thermal ellipsoids are drawn at the 30% probability level.)

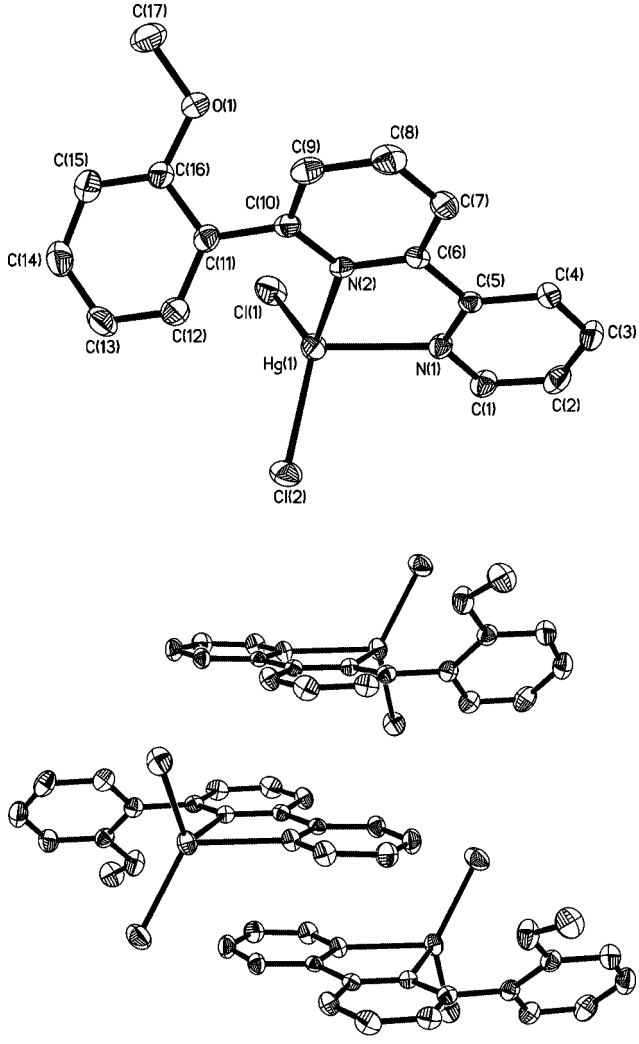


Figure 2. Top: molecular structure of complex **2b**; bottom: the π–π stacking column structure of complex **2b**. (Thermal ellipsoids are drawn at the 30% probability level.)

  

determination were grown from dichloromethane or $CH_3CN$ at room temperature. The ORTEP drawings of the molecular structures of **2a** and **2b** are shown in Figure 1 and Figure 2, respectively. Selected bond lengths and angles for the two complexes are given in Table 1. The X-ray analysis reveals that both complexes adopt a distorted tetrahedral geometry with the metal center chelated by the ligand **1a** through the pyridine nitrogen atoms, and the oxygen atom does not coordinate to the metal center in either complex because of the weak donating ability of the –OMe group. The Zn–N bond lengths in **2a** are 2.071 Å (average), which is close to the values previously reported for similar tetrahedral zinc complexes.[13] In complex **2b**, the two Hg–N bond lengths are slightly different [2.363(3) Å for Hg(1)–N(1) and 2.356(3) Å for Hg(1)–N(2)]. The values are consistent with bond lengths found in other four-coordinate $Hg^{II}$ complexes.[13c,14] The average $M^{II}$–N(pyridyl) bond distances (2.071 Å for Zn–N < 2.359 Å for Hg–N) are consistent with ionic radii. The N–Zn–N bite angle in **2a** [80.27(10)°] is smaller than those found in other pyridyl-containing four-coordinate $Zn^{II}$ complexes,[13a] but larger than the one [70.04(10)°] in its mercury analog **2b**. The dihedral angles between the two pyridyl rings are 10.1° for **2a** and 2.2° for **2b**, and the dihedral angles between the aromatic ring and the adjacent pyridyl ring are 61.0° for **2a** and 50.7° for **2b**. The data of the dihedral angles in two complexes indicate that the conjugated extent of **2b** is larger than that of **2a**. In addition, there is π–π stacking between the pyridyl rings of two neighboring molecules for complex **2a** in the solid state, forming an antiparallel dimeric structure (Figure 1 bottom). The distance between two pyridyl planes is 3.51 Å.[15] In contrast, a π–π stacking column structure was observed in **2b** (Figure 2 bottom). In the column each molecule of **2b** forms antiparallel π–π stacking with two adjacent molecules. The distances between the stacked aromatic planes are 3.46 Å and 3.50 Å, respectively. A similar π–π stacking column structure was also observed in $Hg^{II}$ complexes.[13c]

Table 1. Selected bond lengths (Å) and bond angles (°) for complexes **2a**–**2d**.

| | | | |
|---|---|---|---|
| Complex **2a** | | | |
| Zn(1)–N(1) | 2.079(2) | N(1)–Zn(1)–Cl(1) | 123.53(8) |
| Zn(1)–N(2) | 2.062(2) | N(2)–Zn(1)–Cl(2) | 115.07(8) |
| Zn(1)–Cl(1) | 2.2042(10) | N(1)–Zn(1)–Cl(2) | 108.76(7) |
| Zn(1)–Cl(2) | 2.2104(10) | Cl(1)–Zn(1)–Cl(2) | 117.18(4) |
| N(2)–C(1) | 1.333(4) | C(1)–N(2)–Zn(1) | 125.8(2) |
| N(1)–C(10) | 1.342(4) | C(5)–N(2)–Zn(1) | 113.69(19) |
| N(2)–Zn(1)–N(1) | 80.27(10) | C(10)–N(1)–Zn(1) | 127.7(2) |
| N(2)–Zn(1)–Cl(1) | 106.30(8) | C(6)–N(1)–Zn(1) | 113.09(19) |
| Complex **2b** | | | |
| Hg(1)–N(1) | 2.363(3) | N(1)–Hg(1)–Cl(1) | 118.49(9) |
| Hg(1)–N(2) | 2.356(3) | N(2)–Hg(1)–Cl(2) | 116.07(8) |
| Hg(1)–Cl(1) | 2.3791(14) | N(1)–Hg(1)–Cl(2) | 100.44(9) |
| Hg(1)–Cl(2) | 2.4140(12) | Cl(1)–Hg(1)–Cl(2) | 122.98(4) |
| N(1)–C(1) | 1.344(5) | C(6)–N(2)–Hg(1) | 116.8(2) |
| N(2)–C(10) | 1.344(5) | C(10)–N(2)–Hg(1) | 123.1(2) |
| N(2)–Hg(1)–N(1) | 70.74(10) | C(5)–N(1)–Hg(1) | 116.9(2) |
| N(2)–Hg(1)–Cl(1) | 115.30(8) | C(1)–N(1)–Hg(1) | 123.6(3) |
| Complex **2c** | | | |
| Zn(1)–N(1) | 2.1413(16) | N(2)–Zn(1)–N(3) | 84.17(6) |
| Zn(1)–N(2) | 2.1425(16) | N(2)–Zn(1)–Cl(2) | 118.54(5) |
| Zn(1)–N(3) | 2.3076(16) | N(2)–Zn(1)–Cl(1) | 122.65(5) |
| Zn(1)–Cl(2) | 2.2454(8) | Cl(2)–Zn(1)–N(3) | 97.37(5) |
| Zn(1)–Cl(1) | 2.3066(7) | Cl(1)–Zn(1)–N(3) | 91.39(4) |
| N(1)–Zn(1)–N(2) | 76.34(6) | Cl(2)–Zn(1)–N(3) | 97.37(5) |
| Cl(2)–Zn(1)–Cl(1) | 118.74(3) | Cl(1)–Zn(1)–N(3) | 91.39(4) |
| N(1)–Zn(1)–N(3) | 157.87(6) | C(1)–N(1)–Zn(1) | 125.53(14) |
| Complex **2d** | | | |
| Hg–N(1) | 2.381(10) | N(2)–Hg–N(3) | 76.9(3) |
| Hg–N(2) | 2.440(9) | N(1)–Hg–Cl(2) | 112.4(2) |
| Hg–N(3) | 2.584(10) | Cl(2)–Hg–N(2) | 113.2(2) |
| Hg–Cl(1) | 2.440(3) | N(1)–Hg–Cl(1) | 91.4(2) |
| Hg–Cl(2) | 2.406(3) | N(2)–Hg–Cl(1) | 121.9(2) |
| N(1)–Hg–N(2) | 68.8(3) | Cl(2)–Hg–N(3) | 99.1(2) |
| Cl(1)–Hg–Cl(2) | 124.77(13) | Cl(1)–Hg–N(3) | 89.9(2) |
| N(1)–Hg–N(3) | 140.1(3) | C(1)–N(1)–Hg | 121.3(9) |

The molecular structures of complexes **2c** and **2d** are given in Figure 3 and Figure 4, respectively. Important bond lengths and angles are listed in Table 1. The crystal structure analysis reveals that complexes **2c** and **2d** are five-coordinate and adopt distorted trigonal bipyramidal geometry for the metal center. The ligand **1b** binds to the metal center in tridentate form by three nitrogen atoms, and there-

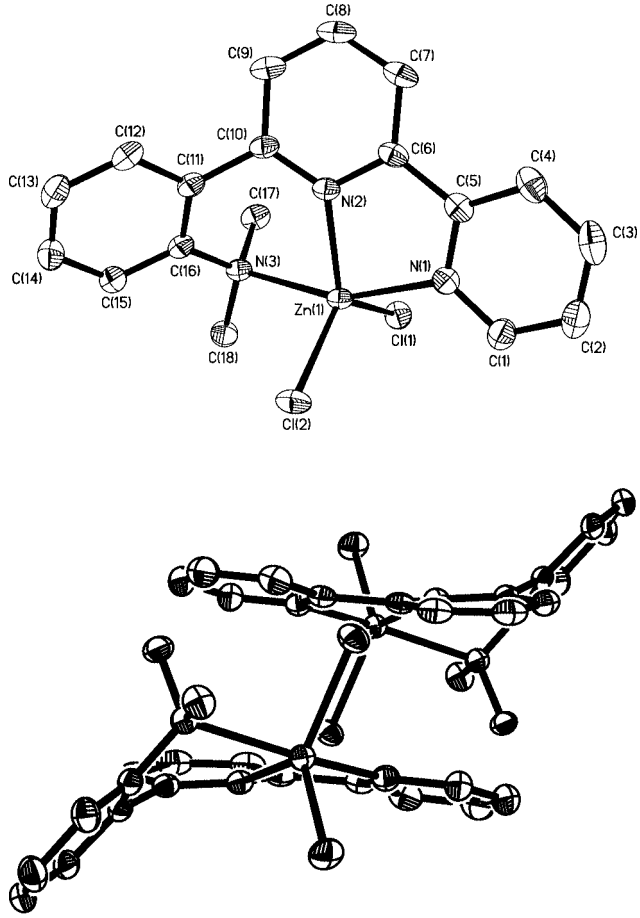


Figure 3. Top: molecular structure of complex **2c**; bottom: the π–π stacking dimer structure of complex **2c**. (Thermal ellipsoids are drawn at the 30% probability level.)

  

fore a five-membered metallacycle and a six-membered metallacycle are constructed. The N(1)–Zn(1)–N(2), N(2)–Zn(1)–N(3), and Cl(1)–Zn(1)–Cl(2) angles are 76.34(6), 84.17(6), and 118.74(3)° in **2c**, respectively. The Zn–N bond lengths, ranging from 2.1413(16) Å [Zn(1)–N(1)] to 2.3076(16) Å [Zn(1)–N(3)], are within the range of 2.098–2.321 Å observed for similar complexes,[16] while they are longer than those (2.079 and 2.062 Å) in the four-coordinate complex **2a**. The dihedral angles between the two pyridyl rings, and between the pyridyl ring and the adjacent aromatic ring are 18.0° and 47.7° for **2c** and 19.1° and 56.3° for **2d**, respectively. In solid state, molecules of **2c** are paired up through intermolecular π–π stacking of the ligand, resulting in the formation of a dimeric structure (Figure 3, bottom). The distance between the planes of the π–π stacked ligand is 3.53 Å. Similar to complex **2b**, a π–π stacking column structure was also observed in the mercury complex **2d** (Figure 4, bottom). The distances between the stacked aromatic planes are 3.42 and 3.65 Å, respectively. The intermolecular π–π interactions suggest that complexes **2a**–**2d** can possess charge transport property, which is essential for electroluminescent material.[17]

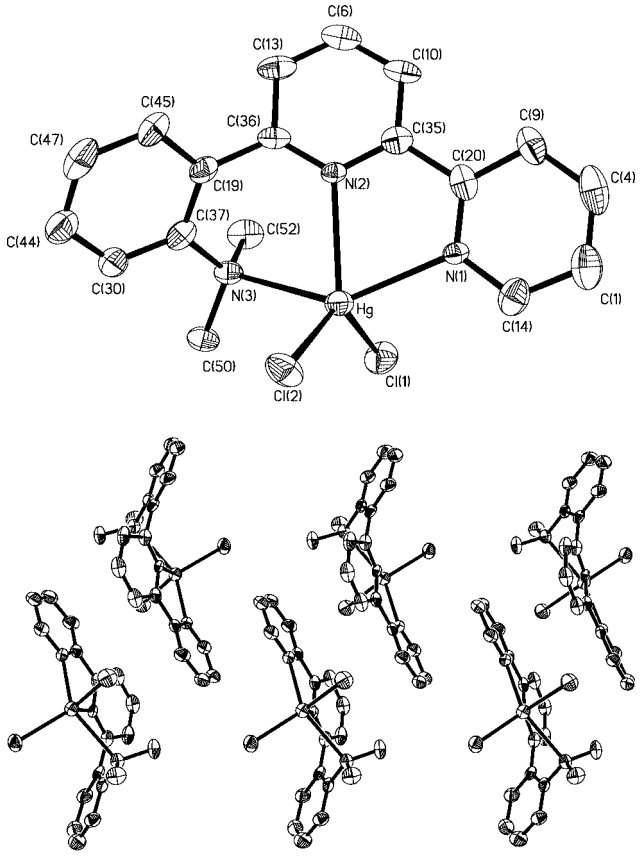


Figure 4. Top: molecular structure of complex **2d**; bottom: the π–π stacking column structure of complex **2d**. (Thermal ellipsoids are drawn at the 30% probability level.)

## Luminescence Properties

Table 2 summarizes the UV/Vis and fluorescent properties of compounds **1a**, **1b** and **2a**–**2d** determined in both solution and the solid state. In solution, the free ligands **1a** and **1b** have emission bands at $\lambda_{max}$ = 431 and 396 nm, respectively. In comparison with the free ligand **1a**, complexes **2a** and **2b** in solution give a broad emission band (bandwidth at half-height = 80–95 nm) with $\lambda_{max}$ = 447 nm and 452 nm, respectively, as shown in Figure 5. The emission maxima of the two complexes are slightly red-shifted compared to that of the free ligand. In contrast to complexes **2a** and **2b**, the emission maxima of **2c** and **2d** in solution are almost the same as that of the free ligand **1b** (see Figure 6). The luminescence of these complexes should be attributed to the transition from π* to π of their ligands. In solution, complex **2a** shows a strongly solvent-dependent emission band and its emission maximum shifts toward a shorter wavelength with the increase in polarity of the solvent. As shown in Figure 7, the emission maximum of **2a** is 461 nm in dichloromethane, while it becomes 358 nm in the polar solvent DMF. This is a rare case, as a red-shift of the emission maximum would be expected for most compounds when solvent polarity increases. The observed blue-shift phenomenon might be attributed to the presence of a highly polarized ground state.[18] The quantum yields of all compounds have been determined in solution. It was found that the quantum yields of the $Zn^{II}$ complexes **2a** and **2c** are slightly higher than those of their free ligands, while the quantum yields of the $Hg^{II}$ complexes **2b** and **2d** are lower than those of their free ligands. These results can be easily understood considering the following factors: the ligand becomes more rigid after coordination with a metal atom, which can reduce the loss of energy by vibrational motions and therefore increase the emission efficiency. On the other hand, the $Hg^{II}$ cation and the chloride anions can quench the fluorescence and result in luminescence decay. The quantum yields of complexes **2a** and **2b** are similar to those of four-coordinate zinc(II) complexes.[13b] The efficiency of **1a** and its corresponding complexes is about 20 times higher than that of **1b** and its corresponding complexes, probably because, in comparison with the –OMe group, the bulkier $–NMe_2$ group reduces the conjugated length and increases vibrational motion in **1b**, **2c**, and **2d**. The emission spectra of compounds **1a**, **1b**, **2a**, **2b**, and **2c** in the solid state are

Table 2. Photoluminescent data for ligands **1a** and **1b** and complexes **2a**–**2d**.

| | Abs. λ (nm) | Ex λ (nm) | Em λ (nm) | Quantum yields[a] | Conditions |
|---|---|---|---|---|---|
| **1a** | 273, 313 | 374 | 431 | 0.108 | $CHCl_3$, 298 K |
| | | | 458, 536 | | solid, 298 K |
| **1b** | 275, 310 | 340 | 394 | 0.005 | $CHCl_3$, 298 K |
| | | | 444 | | solid, 298 K |
| **2a** | 340, 356 | 374 | 447 | 0.113 | $CHCl_3$, 298 K |
| | | | 397 | | solid, 298 K |
| **2b** | 339, 353 | 374 | 452 | 0.083 | $CHCl_3$, 298 K |
| | | | 410 | | solid, 298 K |
| **2c** | 309, 343 | 340 | 395 | 0.006 | $CHCl_3$, 298 K |
| | | | 564 | | solid, 298 K |
| **2d** | 305, 340 | 340 | 394 | 0.003 | $CHCl_3$, 298 K |

[a] Determined using quinine sulfate in sulfuric acid (0.1 M) as a standard in DMF at ambient temperature.

  

shown in Figure 8. Except for **2d**, all compounds in solid state emit bright fluorescence when irradiated by exciting light. The emission maxima of **1a**, **2a**, and **2b** are 536, 397, and 410 nm, respectively. The emission maxima of **2a** and **2b** in the solid state are blue-shifted compared to emission maximum of their ligand **1a**, while the emission maximum of complex **2c** ($\lambda_{max}$ = 564 nm) in the solid state is red-shifted compared to that ($\lambda_{max}$ = 444 nm) of its corresponding ligand **1b**. These properties are probably a result of their π-stacking structures in the solid state.

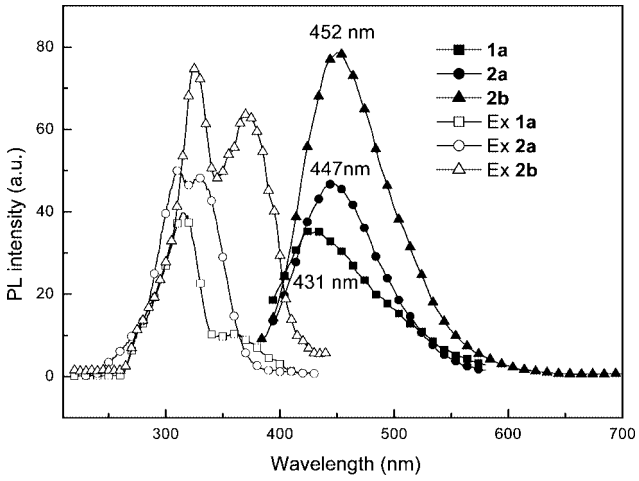


Figure 5. Excitation and emission spectra of compounds **1a**, **2a**, and **2b** in chloroform (ca. $1 \times 10^{-5}$ M).

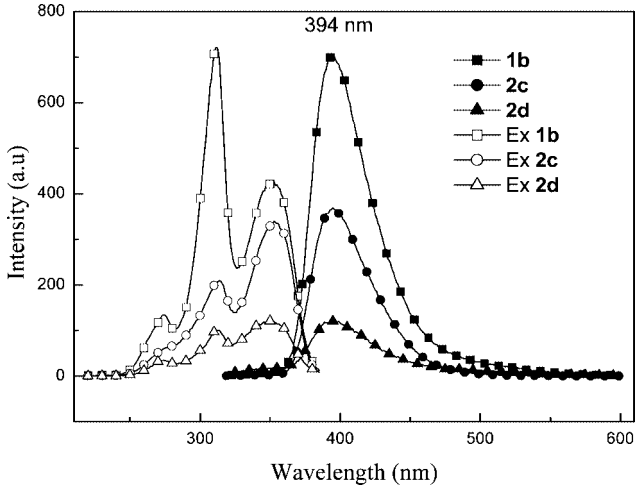


Figure 6. Excitation and emission spectra of compounds **1b**, **2c**, and **2d** in chloroform (ca. $1 \times 10^{-5}$ M).

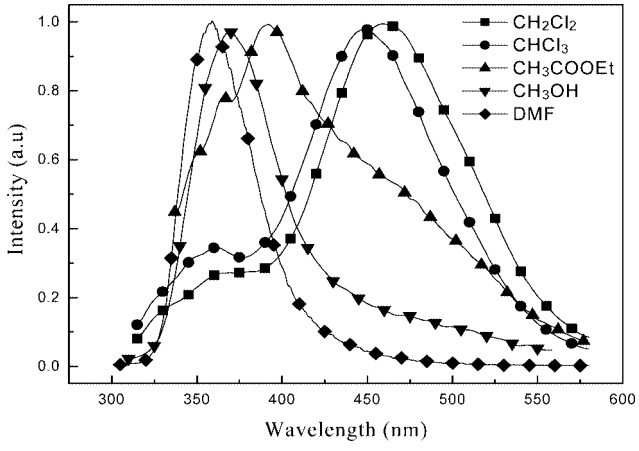


Figure 7. Emission spectra of complex **2a** in various solvents (ca. $1 \times 10^{-5}$ M).

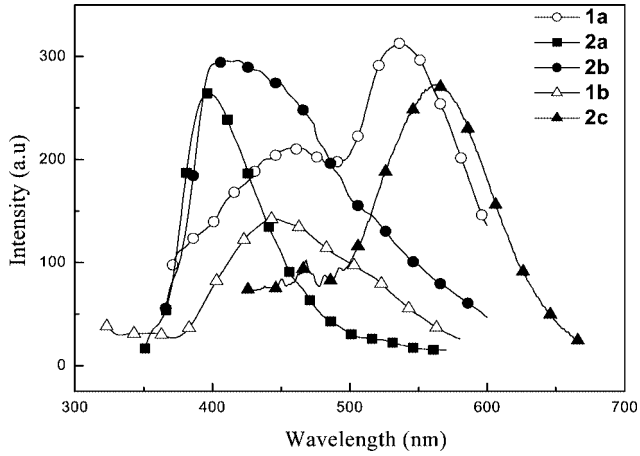


Figure 8. Emission spectra of compounds **1a**, **1b**, **2a**, **2b**, and **2c** in the solid state.

## Conclusions

We have described the syntheses and X-ray structures of a number of d[10] group 12 metal complexes supported by two substituted 2,2′-bipyridine ligands. Crystal structure analysis reveals crystal structures of these complexes are different from each other. It was found that antiparallel dimeric structures are formed for complexes **2a** and **2c** while one-dimensional supramolecular structures are constructed for complexes **2b** and **2d** by π–π stacking in the solid state. These complexes produce fluorescence in both solution and the solid state, and the emission color in the solid state is dramatically affected by their packing structures.

## Experimental Section

All reactions were performed using standard Schlenk techniques in high-purity nitrogen or glovebox techniques. Toluene and diethyl ether were dried by refluxing over sodium and benzophenone and distilled under nitrogen prior to use. $CDCl_3$ was dried with $CaH_2$ for 48 h and vacuum-transferred to an air-free flask. $ZnCl_2$, $HgCl_2$, and *n*BuLi were purchased from Aldrich and used as received. NMR spectra were measured using a Varian Mercury-300 NMR spectrometer. The elemental analysis was performed with a Perkin–Elmer 2400 analyzer. UV/Vis absorption spectra were recorded with a UV-3100 spectrophotometer. Fluorescence measurements were carried out on an RF-5301PC.

**6-[2-(Dimethylamino)phenyl]-2,2′-bipyridine (1b):** A solution of *n*BuLi (30.32 mL, 48.5 mmol) in hexanes was added to a solution of 2-bromo-*N*,*N*-dimethylaniline (9.7 g, 48.5 mmol) in $Et_2O$ (30 mL) under nitrogen at –78 °C. The mixture was allowed to warm to room temperature and stirred overnight. The resulting

  

mixture was added dropwise to an ice-cooled solution of 2,2′-bipyridine (7.57 g, 48.5 mmol) in degassed $Et_2O$ (30 mL), and a wine-red solution was obtained immediately. The resultant mixture was refluxed for 24 h and cooled in an ice bath, then deionized water (25 mL) was added to hydrolyze the products. The yellow organic phase was separated and stirred with $MnO_2$ for 24 h, then filtered and dried with $MgSO_4$. The solid was obtained upon concentration of the solution, and chromatography on silica gel with dichloromethane as eluent afforded a light yellow solid. Yield: 6.7 g (50%). $C_{18}H_{17}N_3$ (275.35): calcd. C 78.52, H 6.22, N 15.26; found C 78.32, H 6.41, N 15.10. $^1$H NMR (300 MHz, $CDCl_3$, 293 K): $\delta$ = 2.77 (s, 6 H, C$H_3$), 7.17 (d, 1 H), 7.32–7.40 (m, 2 H), 7.76–7.84 (m, 4 H), 7.99 (d, 1 H, $J$ = 7.8 Hz), 8.30 (d, 1 H, $J$ = 7.8 Hz), 8.49 (d, 1 H, $J$ = 5.4 Hz), 8.71 (d, 1 H, $J$ = 4.8 Hz) ppm.

**6-(2-Methoxyphenyl)-2,2′-bipyridinezinc Dichloride (2a):** A methanol solution (10 mL) of **1a** (0.2 g, 0.76 mmol) was added to a methanol solution (10 mL) of $ZnCl_2$ (0.11 g, 0.77 mmol). The reaction mixture was stirred for 4 h at room temperature. After filtering, the light yellow precipitate was collected and washed with cold methanol. Pure product was obtained in 81% yield (0.25 g) by recrystallization from $CH_3CN/CH_2Cl_2$. $C_{17}H_{14}Cl_2N_2OZn$ (398.60): calcd. C 51.22, H 3.54, N 7.03; found C 51.40, H 3.67, N 7.15. $^1$H NMR (300 MHz, [$D_6$]DMSO, 293 K): $\delta$ = 3.34 (s, 3 H, C$H_3$), 7.13 (t, 1 H), 7.21 (d, 1 H), 7.41–7.52 (m, 2 H), 7.91–7.99 (m, 4 H), 8.30 (d, 1 H), 8.48 (d, 1 H), 8.72 (d, 1 H) ppm. IR (KBr): $\tilde{\nu}$ = 3072 w, 3007 w, 2959 w, 2850 w, 1600 s, 1569 m, 1484 s, 1459 s, 1441 s, 1401 w, 1299 m, 1260 s, 1248 m, 1179 w, 1162 m, 1119 m, 1055 w, 1023 s, 829 w, 784 s, 755 s, 643 w, 561 w.

**6-(2-Methoxyphenyl)-2,2′-bipyridinemercury Dichloride (2b):** A methanol solution (10 mL) of **1a** (0.2 g, 0.76 mmol) was added to a methanol solution (10 mL) of $HgCl_2$ (0.21 g, 0.77 mmol). The reaction mixture was stirred for 4 h at room temperature. After filtering, the light yellow precipitate was collected and washed with cold methanol. Pure product was obtained in 83% yield (0.34 g) by recrystallization from $CH_3CN$. $C_{17}H_{14}Cl_2HgN_2O$ (533.80): calcd. C 38.25, H 2.64, N 5.25; found C 38.44, H 2.86, N 5.03. $^1$H NMR (300 MHz, [$D_6$]DMSO, 293 K): $\delta$ = 3.35 (s, 3 H, C$H_3$), 7.20 (t, 1 H), 7.23 (d, 1 H), 7.44–7.51 (m, 2 H), 7.91–7.98 (m, 4 H), 8.31 (d, 1 H), 8.47 (d, 1 H), 8.73 (d, 1 H) ppm. IR (KBr): $\tilde{\nu}$ = 3075 w, 3023 w, 2980 w, 2933 w, 2828 w, 1588 s, 1571 m, 1485 s, 1440 s, 1386 m, 1283 m, 1262 s, 1238 s, 1179 m, 1159 m, 1109 m, 1055 w, 1017 s, 1000 s, 946 w, 894 w, 859 w, 824 w, 779 s, 754 s, 734 m, 633 m, 577 w, 616 w.

**6-[2-(Dimethylamino)phenyl]-2,2′-bipyridinezinc Dichloride (2c):** A methanol solution (10 mL) of **1b** (0.2 g, 0.73 mmol) was added to a methanol solution (15 mL) of $ZnCl_2$ (0.11g, 0.74 mmol). The reaction mixture was stirred for 4 h at room temperature. After filtering, the light yellow precipitate was collected and washed with cold methanol. Pure product was obtained in 82% yield (0.25 g) by recrystallization from $CH_3CN/CH_2Cl_2$. $C_{18}H_{17}Cl_2N_3Zn$ (411.64): calcd. C 52.52, H 4.16, N 10.21; found C 52.71, H 4.26, N 10.03. $^1$H NMR (300 MHz, [$D_6$]DMSO, 293 K): $\delta$ = 2.59 (s, 6 H, C$H_3$), 7.13–7.20 (m, 2 H), 7.39 (t, 1 H), 7.52 (s, 1 H), 7.61 (d, 1 H), 7.95–8.13 (m, 3 H), 8.36 (s, 1 H), 8.50 (d, 1 H), 8.71 (d, 1 H) ppm. IR (KBr): $\tilde{\nu}$ = 3061 w, 3015 w, 2984 w, 2928 w, 2873 w, 2833 w, 2362 m, 1601 s, 1568 s, 1446 s, 1401 m, 1298 m, 1262 m, 1246 m, 1156 m, 1130 w, 1104 w, 1053 w, 1021 m, 926 m, 833 m, 783 s, 742 m, 700 w, 655 w, 634 m, 549 w.

**6-[2-(Dimethylamino)phenyl]-2,2′-bipyridinemercury Dichloride (2d):** A methanol solution (10 mL) of **1b** (0.2 g, 0.73 mmol) was added to a methanol solution (15 mL) of $HgCl_2$ (0.21 g, 0.74 mmol). The reaction mixture was stirred for 4 h at room temperature. After filtering, the light yellow precipitate was collected and washed with cold methanol. Pure product was obtained in 85% yield (0.34 g) by

Table 3. Crystal data and structural refinements details for **2a**, **2b**, **2c**, and **2d**.

| | **2a** | **2b** | **2c** | **2d** |
|---|---|---|---|---|
| Empirical formula | $C_{17}H_{14}Cl_2N_2OZn$ | $C_{17}H_{14}Cl_2HgN_2O$ | $C_{18}H_{17}Cl_2N_3Zn$ | $C_{18}H_{17}Cl_2HgN_3$ |
| Formula mass | 398.57 | 533.79 | 411.62 | 546.84 |
| Temp. [K] | 293(2) | 293(2) | 293(2) | 293(2) |
| Wavelength [Å] | 0.71073 | 0.71073 | 0.71073 | 0.71073 |
| Crystal system | monoclinic | monoclinic | monoclinic | triclinic |
| Space group | $P2(1)/n$ | $P2(1)/c$ | $P2(1)/n$ | $P\bar{1}$ |
| $a$ [Å] | 8.2680(17) | 7.5130(15) | 10.236(2) | 8.3858(17) |
| $b$ [Å] | 13.037(3) | 16.718(3) | 13.145(3) | 8.6676(17) |
| $c$ [Å] | 15.433(3) | 13.403(3) | 12.916(3) | 13.173(3) |
| $\alpha$ [°] | 90 | 90 | 90 | 82.56(3) |
| $\beta$ [°] | 95.03(3) | 97.02(3) | 90.08(3) | 89.46(3) |
| $\gamma$ [°] | 90 | 90 | 90 | 73.93(3) |
| $V$ [Å$^3$] | 1657.1(6) | 1670.8(6) | 1737.9(6) | 912.0(3) |
| $Z$ | 4 | 4 | 2 | 2 |
| $D_{calcd.}$ [Mg m$^{-3}$] | 0.799 | 1.061 | 0.787 | 1.991 |
| $F$(000) | 404 | 504 | 420 | 520 |
| Crystal size (mm) | 0.23 × 0.17 × 0.16 | 0.34 × 0.15 × 0.12 | 0.20 × 0.17 × 0.11 | 0.28 × 0.19 × 0.13 |
| $\theta$ range for data collection [°] | 3.08–27.47 | 2.99–27.45 | 3.10–27.46 | 3.00–27.48 |
| Limiting indices | $-10 \le h \le 10$ | $-8 \le h \le 9$ | $-13 \le h \le 11$ | $-9 \le h \le 10$ |
| | $-16 \le k \le 16$ | $-21 \le k \le 21$ | $-17 \le k \le 17$ | $-10 \le k \le 11$ |
| | $-20 \le l \le 17$ | $-17 \le l \le 17$ | $-16 \le l \le 16$ | $-17 \le l \le 17$ |
| Data/restraints/parameters | 3774/0/208 | 3746/0/264 | 3973/0/285 | 3979/0/217 |
| Goodness-of-fit on $F^2$ | 1.079 | 1.004 | 1.055 | 1.102 |
| Final $R$ indices [$I > 2\sigma(I)$] | $R_1$[a] = 0.0414 | $R_1$[a] = 0.0260 | $R_1$[a] = 0.0280 | $R_1$[a] = 0.0663 |
| | $wR_2$[b] = 0.1193 | $wR_2$[b] = 0.0580 | $wR_2$[b] = 0.0670 | $wR_2$[b] = 0.1439 |
| $R$ indices (all data) | $R_1$[a] = 0.0487 | $R_1$[a] = 0.0342 | $R_1$[a] = 0.0371 | $R_1$[a] = 0.0823 |
| | $wR_2$[b] = 0.1222 | $wR_2$[b] = 0.0614 | $wR_2$[b] = 0.0707 | $wR_2$[b] = 0.1517 |
| Largest diff. peak/hole [e Å$^{-3}$] | 0.665, –0.261 | 0.917, –1.172 | 0.315, –0.231 | 2.854, –1.997 |

[a] $R_1 = \Sigma||F_o| - |F_c||/\Sigma|F_o|$. [b] $wR_2 = [\Sigma[w(F_o^2 - F_c^2)^2]/\Sigma[w(F_o^2)^2]]^{1/2}$.

  

recrystallization from $CH_3CN/CH_2Cl_2$. $C_{18}H_{17}Cl_2HgN_3$ (546.84): calcd. C 39.53, H 3.13, N 7.68; found C 39.32, H 3.26, N 7.89. $^1H$ NMR (300 MHz, [D$_6$]DMSO, 293 K): $\delta$ = 2.58 (s, 6 H, C$H_3$), 7.15–7.21 (m, 2 H), 7.41 (s, 1 H), 7.58 (m, 2 H), 7.98–8.09 (m, 3 H), 8.41 (s, 1 H), 8.53 (d, 1 H), 8.72 (d, 1 H) ppm. IR (KBr): $\tilde{\nu}$ = 3064 w, 3013 w, 2964 w, 2869 w, 2835 w, 2795 w, 2364 w, 1594 s, 1568 s, 1443 s, 1288 m, 1259 w, 1233 w, 1185 m, 1159 m, 1126 w, 1110 w, 1049 w, 1008 m, 931 m, 891 w, 826 m, 777 s, 696 w, 630 m, 561 w, 543 w.

**X-ray Structure Determinations of 2a, 2b, 2c, and 2d:** Single crystals of **2a**, **2b**, **2c**, and **2d** suitable for X-ray structural analysis were obtained from dichloromethane or $CH_3CN$. Diffraction data were collected at 293 K on a Rigaku R-AXIS RAPID IP diffractometer equipped with graphite-monochromated Mo-$K_\alpha$ radiation ($\lambda$ = 0.71073 Å) for **2a**, **2b**, **2c**, and **2d**. Details of the crystal data, data collections, and structure refinements are summarized in Table 3. The structures were solved by direct methods[19] and refined by full-matrix least-squares on $F^2$. All non-hydrogen atoms were refined anisotropically and the hydrogen atoms were included in idealized position. All calculations were performed using the SHELXTL[20] crystallographic software packages. For **2d**, the final difference maps revealed residual electron density near the mercury atoms (2.85 and 2.81 e Å$^{-3}$) but no regions of electron density that could be attributed to additional atomic sites.

CCDC-602363 (for **2a**), -602364 (for **2b**), -602365 (for **2c**), and -602366 (for **2d**) contain the supplementary crystallographic data for this paper. These data can be obtained free of charge from The Cambridge Crystallographic Data Centre via www.ccdc.cam.ac.uk/data_request/cif.

## Acknowledgments

This work was supported by the National Natural Science Foundation of China (No. 20374023) and Ministry of Science and Technology of China (No. 2002CB6134003).

[1] a) C. W. Tang, S. A. Vanslyke, *Appl. Phys. Lett.* **1987**, *51*, 913–915; b) S. N. Wang, *Coord. Chem. Rev.* **2001**, *215*, 79–98; c) C. H. Chen, J. Shi, *Coord. Chem. Rev.* **1998**, *171*, 161–174; d) F. Li, M. Zhang, G. Cheng, J. Feng, Y. Zhao, Y. G. Ma, S. Y. Liu, J. C. Shen, *Appl. Phys. Lett.* **2004**, *84*, 148–150; e) Q. S. Zhang, Q. G. Zhou, Y. X. Cheng, L. X. Wang, D. G. Ma, X. B. Jing, F. S. Wang, *Adv. Mater.* **2004**, *16*, 432–436; f) G. B. Cunningham, Y. T. Li, S. X. Liu, K. S. Schanze, *J. Phys. Chem. B* **2003**, *107*, 12569–12572.

[2] a) T. H. Kwon, H. S. Cho, M. K. Kim, J. W. Kim, J. J. Kim, K. H. Lee, S. J. Park, I. S. Shin, H. Kim, D. M. Shin, Y. K. Chung, J. I. Hong, *Organometallics* **2005**, *24*, 1578–1585; b) F. M. Hwang, H. Y. Chen, P. S. Chen, C. S. Liu, Y. Chi, C. F. Shu, F. L. Wu, P. T. Chou, S. M. Peng, G. H. Lee, *Inorg. Chem.* **2005**, *44*, 1344–1353; c) J. Li, P. I. Djurovuch, B. D. Alleyne, M. Yousufuddin, N. N. Ho, J. C. Thomas, J. C. Peters, R. Bau, M. E. Thompson, *Inorg. Chem.* **2005**, *44*, 1713–1727; d) X. M. Liu, W. Gao, Y. Mu, G. H. Li, L. Ye, H. Xia, Y. Ren, S. H. Feng, *Organometallics* **2005**, *24*, 1614–1619.

[3] a) V. A. Montes, G. Li, R. Pohl, J. Shinar, P. Anzenbacher Jr, *Adv. Mater.* **2004**, *16*, 2001–2003; b) R. Pohl, V. A. Montes, J. Shinar, P. Anzenbacher Jr, *J. Org. Chem.* **2004**, *69*, 1723–1725; c) R. Pohl, P. Anzenbacher Jr, *Org. Lett.* **2003**, *5*, 2769–2772.

[4] a) Q. G. Wu, J. A. Lavigne, Y. Tao, M. D'Iorio, S. N. Wang, *Inorg. Chem.* **2000**, *39*, 5248–5254; b) Q. G. Wu, A. Hook, S. N. Wang, *Angew. Chem. Int. Ed.* **2000**, *39*, 3933–3935; c) D. T. Song, S. N. Wang, *Eur. J. Inorg. Chem.* **2003**, 3774–3782; d) Q. G. Wu, J. A. Lavigne, Y. Tao, M. D'Iorio, S. N. Wang, *Chem. Mater.* **2001**, *13*, 17–77.

[5] a) Y. Liu, J. H. Guo, H. D. Zhang, Y. Wang, *Angew. Chem. Int. Ed.* **2002**, *41*, 182–184; b) Y. Q. Li, Y. Liu, W. M. Bu, J. H. Guo, Y. Wang, *Chem. Commun.* **2000**, 1551–1552.

[6] a) W. K. Chan, P. K. Ng, X. Gong, S. J. Hou, *Appl. Phys. Lett.* **1999**, *753*, 3920–3922; b) K. Z. Wang, L. Huang, L. H. Gao, L. P. Jin, C. H. Huang, *Inorg. Chem.* **2002**, *41*, 3353–3358; c) S. Ranjan, S. Y. Lin, K. C. Hwang, Y. Chi, W. L. Ching, C. S. Liu, Y. T. Tao, C. H. Chien, S. M. Peng, G. H. Lee, *Inorg. Chem.* **2003**, *42*, 1248–1255; d) F. Li, M. Zhang, G. Cheng, J. Feng, Y. Zhao, Y. G. Ma, S. Y. Liu, J. C. Shen, *Appl. Phys. Lett.* **2004**, *84*, 148–150.

[7] a) Y. L. Tung, S. W. Lee, Y. Chi, L. S. Chen, C. F. Shu, F. I. Wu, A. J. Carty, P. T. Chou, S. M. Peng, G. H. Lee, *Adv. Mater.* **2005**, *17*, 1059–1063; b) H. Xia, C. Zhang, X. Liu, S. Qiu, P. Lu, F. Shen, J. Zhang, Y. Ma, *J. Phys. Chem. B* **2004**, *108*, 3185–3190; c) H. Xia, C. Zhang, S. Qiu, P. Lu, J. Zhang, Y. Ma, *Appl. Phys. Lett.* **2004**, *84*, 290–292.

[8] a) B. Carlson, G. D. Phelan, W. Kaminsky, L. Dalton, X. Z. Jiang, S. Liu, A. K.-Y. Jen, *J. Am. Chem. Soc.* **2002**, *124*, 14162–14172; b) Y. L. Chen, S. W. Lee, Y. Chi, K. C. Hwang, S. B. Kumar, Y. H. Hu, Y. M. Cheng, P. T. Chou, S. M. Peng, G. H. Lee, S. J. Yeh, C. T. Chen, *Inorg. Chem.* **2005**, *44*, 4287–4294; c) Y. L. Tung, P. C. Wu, C. S. Liu, Y. Chi, J. K. Yu, Y. H. Hu, P. T. Chou, S. M. Peng, G. H. Lee, Y. Tao, J. C. Arthur, C. F. Shu, F. I. Wu, *Organometallics* **2004**, *23*, 3745–3748..

[9] a) Y. G. Ma, C. M. Che, H. Y. Chao, X. M. Zhou, W. H. Chan, J. C. Shen, *Adv. Mater.* **1999**, *11*, 852–857; b) X. M. Zhang, M. L. Tong, M. L. Gong, H. K. Lee, L. Luo, K. F. Li, Y. X. Tong, X. M. Chen, *Chem. Eur. J.* **2002**, *8*, 3187–3194; c) G. Yu, S. W. Yin, Y. Q. Liu, Z. G. Shuai, D. B. Zhu, *J. Am. Chem. Soc.* **2003**, *125*, 14816–14824.

[10] a) W. K. Lo, W. K. Wong, W. Y. Wong, J. P. Guo, *Eur. J. Inorg. Chem.* **2005**, 3950–3954; b) M. R. Haneline, M. Tsunoda, F. P. Gäbbai, *J. Am. Chem. Soc.* **2002**, *124*, 3737–3742; c) R. Q. Fan, D. S. Zhu, Y. Mu, G. H. Li, Y. L. Yang, Q. Su, *Eur. J. Inorg. Chem.* **2004**, 4891–4897.

[11] a) V. W. W. Yam, K. K. W. Lo, W. K. M. Fung, C. R. Wang, *Coord. Chem. Rev.* **1998**, *171*, 17–41; b) H. H. Patterson, S. M. Kanan, M. A. Omary, *Coord. Chem. Rev.* **2000**, *208*, 227–241.

[12] a) M. Schmittel, C. Michel, A. Wiegrefe, V. Kalsani, *Synthesis* **2001**, 1561–1567; b) C. C. Kwok, H. M. Y. Ngai, S. C. Chan, I. H. T. Sham, C. M. Che, N. Y. Zhu, *Inorg. Chem.* **2005**, *44*, 4442–4444.

[13] a) Q. G. Wu, J. A. Lavigne, Y. Tao, M. D'Iorio, S. N. Wang, *Inorg. Chem.* **2000**, *39*, 5248–5254; b) K. Y. Ho, W. Y. Yu, K. K. Cheung, C. M. Che, *J. Chem. Soc., Dalton Trans.* **1999**, 1581–1586; c) Q. D. Liu, R. Y. Wang, S. N. Wang, *Dalton Trans.* **2004**, 2073–2079.

[14] a) S. M. Berry, D. C. Bebout, R. J. Butcher, *Inorg. Chem.* **2005**, *44*, 27–39; b) S. L. Zheng, J. P. Zhang, X. M. Chen, Z. L. Huang, Z. Y. Lin, W. T. Wong, *Chem. Eur. J.* **2003**, *9*, 3888–3896.

[15] C. Janiak, *J. Chem. Soc., Dalton Trans.* **2000**, 3885–3896.

[16] a) R. Q. Fan, D. S. Zhu, H. Ding, Y. Mu, Q. Su, H. Xia, *Synth. Met.* **2005**, *149*, 135–141; b) S. G. Liu, J. L. Zuo, Y. Wang, Y. Z. Li, X. Z. You, *J. Phys. Chem. Solids* **2005**, *66*, 735–740; c) S. Das, C. H. Hung, S. Goswami, *Inorg. Chem.* **2003**, *42*, 5153–5157.

[17] Y. Q. Li, Y. Liu, W. M. Bu, D. Lu, Y. Wu, Y. Wang, *Chem. Mater.* **2000**, *12*, 2672–2675.

[18] E. M. Kosower, *J. Am. Chem. Soc.* **1958**, *80*, 3253–3260.

[19] *SHELXTL*, PC Siemens Analytical X-ray Instruments, Madison, WI, **1993**.

[20] G. M. Sheldrick, *SHELXTL Structure Determination Programs*, Version 5.0, PC Siemens Analytical Systems, Madison, WI, **1994**.

Received: March 25, 2006
Published Online: August 24, 2006

  